

# Mode-selective vibrational excitation induced by nonequilibrium transport processes in single-molecule junctions

Rainer Härtle<sup>(a)</sup>, Roie Volkovich<sup>(b)</sup>, Michael Thoss<sup>(a)</sup>, and Uri Peskin<sup>(b)</sup>

<sup>(a)</sup>*Institut für Theoretische Physik and Interdisziplinäres Zentrum für Molekulare Materialien,  
Friedrich-Alexander-Universität Erlangen-Nürnberg,  
Staudtstr. 7/B2, D-91058 Erlangen, Germany*

<sup>(b)</sup>*Schulich Faculty of Chemistry,  
and the Lise Meitner Center for Computational Quantum Chemistry  
Technion-Israel Institute of Technology, Haifa 32000, Israel*

## Abstract

In a nanoscale molecular junction at finite bias voltage, the intra-molecular distribution of vibrational energy can strongly deviate from the thermal equilibrium distribution and specific vibrational modes can be selectively excited in a controllable way, regardless of the corresponding mode frequency. This is demonstrated for generic models of asymmetric molecular junctions with localized electronic states, employing a master equation as well as a nonequilibrium Green's function approach. It is shown that the applied bias voltage controls the excitation of specific vibrational modes coupled to these states, by tuning their electronic population, which influences the efficiency of vibrational cooling processes due to energy exchange with the leads.

Nonequilibrium processes in nanoscale quantum systems and particularly quantum transport processes in molecular junctions [1, 2] have received great attention recently. Coupling a single molecule to two metal or semi-conductor electrodes at different electrochemical potentials drives it into a nonequilibrium steady-state which can deviate significantly from thermal equilibrium. The mechanical stability of such a junction and its transport properties strongly depend on the distribution of vibrational energy between the different molecular modes. Experiments employing scanning tunneling microscopy (STM) [3–5] or molecular junctions [6–8] as well as theoretical studies [9–17] indeed demonstrated nonequilibrium vibrational excitation, as well as conformational changes and chemical reactions induced by charge transport under finite bias.

In this communication we demonstrate that the molecular junction scenario offers a new route to mode-selective excitations of molecules. Mode-selective excitations were discussed extensively in the past in the context of photo-induced chemical reactions [18–20]. The original idea was that energy can be directed into specific mode-excitation or bond-cleavage, prior to its statistical randomization due to internal vibrational energy redistribution (IVR) processes. Since statistical distribution of energy usually prevails in polyatomic molecules and in molecules in condensed phase environments, typically the lower frequency modes are excited and the weaker bonds are broken. The challenge of overcoming this statistical behavior led to control schemes based on laser excitations [21–23]. While the excitation of a molecule with a laser pulse results in transient nonequilibrium dynamics followed by relaxation to equilibrium, in a biased molecular junction a stationary nonequilibrium state is maintained.

The external bias voltage, as we will show, can be used to drive the molecule into different nonequilibrium internal energy distributions, thus enabling voltage-controlled selective excitations of specific vibrational motions, conformational changes or, in principle, bond dissociation. While differences in symmetry between different vibrational modes lead to well known selection and/or propensity rules [24, 25] for excitations, in this work we focus on bias-controlled selective excitations induced by nonequilibrium effects and use a simple model to demonstrate how non-thermal excitations of specific molecular modes can be independently controlled by the bias voltage.

To demonstrate and analyze the possibility of mode-selective vibrational excitation, we consider here a representative model for vibronic coupling in an asymmetric molecular junc-

tion. The model, schematically depicted in Fig. 1, comprises two electronic states on the molecular bridge, which are assumed to be localized at different parts of the molecule. This localization can be achieved, *e.g.*, employing electron donating or withdrawing functional side groups as illustrated in Fig. 1, and results in an asymmetry in the coupling of the electronic states to the leads such that the population of the electronic states can be controlled by the bias direction (see below). Furthermore, due to the asymmetric charge distribution, the coupling of the electronic to the vibrational degrees of freedom will be asymmetric as well, thus allowing for selective current-induced vibrational excitation.

The Hamiltonian describing vibrationally coupled electron transport in this model is given by

$$H = H_M + H_{\text{Leads}} + H_{M,\text{Leads}}, \quad (1)$$

where the different parts correspond to the molecular bridge, the leads, and the molecule-lead coupling, respectively. The molecular part of the Hamiltonian,  $H_M = H_0 + H_B$  with

$$H_0 = \sum_{m=1}^{N_{\text{el}}} \epsilon_m a_m^\dagger a_m + \sum_{\nu=1}^{N_{\text{vib}}} \Omega_\nu c_\nu^\dagger c_\nu + \sum_{\nu=1}^{N_{\text{vib}}} \frac{c_\nu^\dagger + c_\nu}{\sqrt{2}} \sum_{m,m'=1}^{N_{\text{el}}} \lambda_{\nu,m,m'} a_m^\dagger a_{m'}, \quad (2)$$

involves  $N_{\text{el}}$  electronic states on the molecular bridge with energies  $\epsilon_m$  and the corresponding creation and annihilation operators  $a_m^\dagger$  and  $a_m$ . The vibrational degrees of freedom of the molecular bridge ('internal modes') are described by harmonic modes with frequencies  $\Omega_\nu$ , corresponding creation and annihilation operators  $c_\nu^\dagger$  and  $c_\nu$ , and are assumed to be linearly coupled to the electronic degrees of freedom. To incorporate vibrational relaxation effects, each internal vibrational mode is coupled to a thermal bath described by the Hamiltonian

$$H_B = \sum_{\nu=1}^{N_{\text{vib}}} \sum_{\beta_\nu=1}^{N_{\text{bath}}} [\omega_{\beta_\nu} d_{\beta_\nu}^\dagger d_{\beta_\nu} + (c_\nu^\dagger + c_\nu) \eta_{\nu,\beta_\nu} (d_{\beta_\nu}^\dagger + d_{\beta_\nu})]. \quad (3)$$

Here,  $d_{\beta_\nu}^\dagger, d_{\beta_\nu}$  denote the creation and annihilation operator for a bath mode with frequency  $\omega_{\beta_\nu}$ , and  $\eta_{\nu,\beta_\nu}$  is the system-bath coupling strength. All properties of the bath that influence the dynamics of the system are described by the spectral densities  $J_\nu(\omega) = \sum_{\beta_\nu=1}^{N_{\text{bath}}} \eta_{\nu,\beta_\nu}^2 \delta(\omega - \omega_{\beta_\nu})$ . In the calculations presented below, we have assumed an Ohmic bath model, *i.e.*  $J_\nu(\omega) = \frac{\zeta_{\nu}^2}{\omega_{c,\nu}^2} \omega e^{-\omega/\omega_{c,\nu}}$ .

The electrodes are modeled as non-interacting electron reservoirs with electrochemical potential  $\mu_{L/R}$ . The electronic states in the right and left electrodes are characterized by

their energies  $\epsilon_k$ , and the corresponding electron creation and annihilation operators  $b_k^\dagger$  and  $b_k$ , resulting in the Hamiltonian  $H_{\text{Leads}} = \sum_{k \in \text{L,R}} \epsilon_k b_k^\dagger b_k$ . Finally, the molecule-lead coupling is given by  $H_{\text{M,Leads}} = \sum_{k \in \text{L}; m} v_{\text{L},m} \xi_{\text{L},k} a_m^\dagger b_k + \sum_{k \in \text{R}; m} v_{\text{R},m} \xi_{\text{R},k} a_m^\dagger b_k + h.c.$ . Here,  $v_{\text{L/R},m}$  are dimensionless factors that determine the asymmetry in the coupling of the  $m$ th molecular state to the right or the left electrode, and the molecule-lead coupling strengths are defined as  $\xi_{\text{L/R},k}$  and correspond to width functions  $\Gamma_{\text{L/R}}(\epsilon) = 2\pi \sum_{k \in \text{L/R}} |\xi_{\text{L/R},k}|^2 \delta(\epsilon - \epsilon_k)$ . In the calculation presented below the leads are modeled as semi-infinite tight-binding chains, where the width-function for the semielliptic band is  $\Gamma_{\text{L/R}}(\epsilon) \equiv \frac{|\xi|^2}{|\gamma|^2} \sqrt{(2|\gamma|)^2 - (\epsilon - \mu_{\text{L/R}})^2}$  with bandwidth  $4\gamma$  and overall molecule-lead coupling strength  $\xi$ .

Nonequilibrium transport in molecular junctions is studied employing two complementary approaches, where the technical details are summarized in the Supporting Information [26] (see also Refs. 13 and 14). Briefly, the first approach is based on propagating in time a reduced density matrix  $\rho_{\text{S}}(t)$ , which incorporates the electronic states of the molecular bridge, the internal vibrational modes and the vibronic coupling in a non-perturbative manner [27]. A master equation for  $\rho_{\text{S}}(t)$  is obtained employing perturbation theory in the molecule-lead and system-bath coupling as well as the Markov approximation [28–30]. Steady-state observables are determined at the infinite-time limit, *e.g.*, the internal mode excitation is given by  $\langle c_\nu^\dagger c_\nu \rangle = \lim_{t \rightarrow \infty} \text{tr}_{\text{S}}[\rho_{\text{S}}(t) c_\nu^\dagger c_\nu]$ . The second approach is based on nonequilibrium Green's functions (NEGF). Specifically, we have applied a method originally proposed by Galperin *et al.* [12], which was recently extended to account for multiple vibrational modes and multiple electronic states [13, 14]. This approach is complementary to the master equation approach, because it is non-Markovian and non-perturbative in the molecule lead coupling, while vibronic coupling is treated in an approximate non-perturbative way. Thus, the NEGF method provides a more comprehensive description of the interactions between the molecule and the leads, while the master equation approach invokes no explicit approximations with respect to the electron-vibrational coupling. The good agreement of the results presented below demonstrates the validity of both approaches for the selected model parameters. The results also show that coherences between the molecular levels, which are not included in the master equation approach but in the NEGF scheme, are negligible.

Various possible mechanisms can result in mode-selective vibrational excitation. In the following, we discuss mechanisms which are expected to be particularly relevant in nanoscale molecular junctions. In all cases we consider the model described above with two elec-

tronic states, which are coupled asymmetrically to the two electrodes and selectively to two molecular modes, corresponding to  $\lambda_{\nu,m,m'} = \delta_{m,m'}\lambda_{\nu,m}$ , with  $\lambda_{1,2} = \lambda_{2,1} = 0$  in Eq. (2). The specific model parameters are detailed in Table I. We note that the mode-selective vibrational excitation reported below is also obtained for models with small to moderate off-diagonal vibrational coupling terms,  $\lambda_{1,2} = \lambda_{2,1} \lesssim \lambda_{1,1}/10$ , but becomes less efficient for larger off-diagonal coupling strengths.

Fig. 2 shows results for the vibrational excitation of the two internal modes as a function of the applied bias voltage for a model with a moderate coupling of the internal modes to a thermal bath. The results demonstrate that the vibrational excitation of each specific mode depends significantly on the bias voltage and can be controlled by its direction. This finding can be rationalized considering that the effective electronic-vibrational coupling (and thus the vibrational excitation) of a specific mode depends on the residence time of the electrons on the molecule (relative to the vibrational period), and thus on the occupation of the electronic state to which the mode is coupled. The inset of Fig. 2 shows that the occupation of the two electronic states of the asymmetric junction (see Fig. 1) is sensitive to the bias direction, so that in each direction the unoccupied state is associated with lower vibrational excitation.

The mechanism of current-induced vibrational excitation and the dependence on the bias (direction) can be significantly more complex and intriguing if the cooling by the external thermal bath is less effective and other nonequilibrium effects prevail. As an example, Fig. 3 depicts results for a model with a weak coupling to a thermal bath. The results show that the overall vibrational excitation is significantly larger, revealing efficient current-induced heating processes schematically depicted in Fig. 4a. The level of vibrational excitation for the two modes depends again significantly and in a nontrivial way on the bias voltage. The results presented in Fig. 3b for a model where the two vibrational modes have identical frequencies,  $\Omega_1 = \Omega_2$ , and the same vibronic coupling strengths,  $\lambda_{1,1} = \lambda_{2,2}$ , reveal furthermore that this behavior is not solely caused by different vibrational excitation energies or vibronic coupling strengths but rather results from the asymmetry of the molecular junction. It is important to note that the relation between the degree of vibrational excitation of a given mode and the occupation of the electronic state, to which the mode is coupled, is reversed with respect to the results obtained above with a significant coupling to a thermal bath [31] (cf. Fig. 2), *i.e.*, vibrational excitation is less significant for the mode coupled to the

occupied electronic state. This intriguing finding suggests that other cooling mechanisms are active that are selectively associated with the occupied molecular level.

Indeed, in the absence of efficient cooling by a thermal bath the vibrational excitation of the internal modes due to "heating" processes can be limited only by energy loss to the electrons in the leads. One of these cooling mechanisms is provided by the transport process itself, where upon electron transmission from one lead to another a vibrational quantum is absorbed (Fig. 4b), instead of being emitted (Fig. 4a). Notice that when the non-equilibrium vibrational distribution involves significant population of excited states, cooling by phonon absorption becomes as efficient as heating by phonon emission. However, since transport processes depend on the molecular coupling to both of the leads, they are not expected to distinguish between the two electronic states or to selectively influence the respective mode excitation. In contrast, cooling processes that involve only one lead, directly transfer the junction asymmetry to the vibrational system. Two such processes, which involve the creation of an electron-hole pair in the left lead [32] by absorbing a single vibrational quantum [5], are shown in Fig. 4c and Fig. 4d. When the applied bias is sufficiently large,  $\Phi \gtrsim 2\epsilon_{1/2}$ , the asymmetry in the coupling of state 1 and state 2 to the left lead (sketched by the thickness of the transmission arrows in Fig. 4c and Fig. 4d) implies that most of the electron-hole pair creation processes in the left lead involve state 1. As a result of these absorption processes, the mode coupled to state 1 loses significantly more energy to the left lead than the mode coupled to state 2. Similar electron-hole pair creation processes can occur in the right lead as well. However, provided that the two molecular states are located sufficiently above the Fermi energy of the electrodes, electron-hole pair creation in the right lead requires absorption of multiple vibrational quanta and is thus less efficient. The net result is that for positive bias voltages electron-hole pair creation processes in the left electrode provide an exclusive source of cooling for the mode that is coupled to state 1, which is the occupied electronic state. Inverting the bias direction, cooling at the right lead becomes dominant, and again, the mode coupled to the occupied electronic state (mode 2 in this case) is more effectively cooled. The bias direction therefore controls the efficiency of the prominent vibrational cooling mechanism in the junction, and selectively controls the degree of mode excitation. It is noted that this selective vibrational excitation depends on the two electronic states being located sufficiently above the Fermi energy of the electrodes, and thus can be switched off by shifting them towards the Fermi energy.

One therefore has two possibilities to control this mechanism for mode-selective excitation: the direction of the bias voltage, which selects a specific mode, and the gate voltage, which controls the degree of excitation of the selected mode.

In summary, we have demonstrated and analyzed mode-selective vibrational excitation in single-molecule junctions induced by nonequilibrium electron transport. The results obtained here for a generic model show that necessary prerequisites for mode-selectivity in molecular junctions involve asymmetry of the molecule-lead coupling and/or the charge distribution as well as state-dependent vibronic coupling. This can be controlled in a molecular junction by choosing appropriate functional and/or anchor groups. The ability to use the external bias in order to direct energy selectively into a given molecular vibrational mode suggests the possibility of mode-selective chemistry, *e.g.* the cleavage of a specific, not necessarily the weakest, chemical bond induced by nonequilibrium transport processes.

### Acknowledgments

This research was supported by the German-Israeli Foundation for scientific development (GIF).

### References

- 
- [1] C. Joachim and S. Roth, *Atomic and molecular wires* (Kluwer, Dordrecht, 1997).
  - [2] A. Nitzan and M. A. Ratner, *Science* 300, 1384 (2003).
  - [3] J. I. Pascual *et al.*, *Nature* 423, 525 (2003).
  - [4] B.-Y. Choi *et al.*, *Phys. Rev. Lett.* 96, 156106 (2006).
  - [5] G. Schulze *et al.*, *Phys. Rev. Lett.* 100, 136801 (2008).
  - [6] Z. Ioffe *et al.*, *Nature Nanotech.* 3, 727 (2008).
  - [7] H. Park *et al.*, *Nature* 407, 57-60 (2000).
  - [8] H. Song *et al.*, *Appl. Phys. Lett.* 94, 103110 (2009)
  - [9] A. Mitra *et al.*, *Phys. Rev. B* 69, 245302 (2004).
  - [10] J. Koch *et al.*, *Phys. Rev. B* 73, 155306 (2006).
  - [11] J. Koch and F. von Oppen, *Phys. Rev. Lett.* 94, 206804 (2005).
  - [12] M. Galperin *et al.*, *Phys. Rev. B* 73, 045314 (2006).
  - [13] R. Härtle *et al.*, *Phys. Rev. B* 77, 205314 (2008).

- [14] R. Härtle *et al.*, Phys. Rev. Lett. 102, 146801 (2009).
- [15] V. May and O. Kühn, Chem. Phys. Lett. 420, 192 (2006).
- [16] C-C. Kaun and T. Seideman, Phys. Rev. Lett. 94, 226801 (2005).
- [17] A. Hackl *et al.*, Phys. Rev. Lett. 102, 196601 (2009)
- [18] J. Jortner *et al.*, *Mode selective chemistry*, (Kluwer, Amsterdam, 1991).
- [19] Z. Liu *et al.*, Science 312, 1024 (2006).
- [20] F. F. Crim, P. N. A. S. USA 105, 12654 (2008).
- [21] E. D. Potter *et al.*, Nature 355, 66 (1992).
- [22] R. N. Zare, Science 279, 1875 (1998).
- [23] P. W. Brumer and M. Shapiro, *Principles of the Quantum Control of Molecular Processes*, (Wiley, 2003).
- [24] A. Troisi and M. A. Ratner, Nano Lett. 6, 1784 (2006).
- [25] A. Gagliardi *et al.*, Phys. Rev. B. 75, 174306 (2007).
- [26] See Supplementary Material Document No for details.
- [27] U. Peskin, J. Phys. B: At. Mol. Opt. Phys. 43 (2010).
- [28] D. Egorova *et al.*, J. Chem. Phys. 119, 2761 (2003).
- [29] R. Volkovich *et al.*, J. Chem. Phys. 129, 034501 (2008).
- [30] E. G. Petrov and P. Hänggi, Phys. Rev. Lett. 86, 2862 (2001).
- [31] Except for the small bias region, in which one of the molecular conductance channels is closed
- [32] A different mechanism for electron-hole pair creation, which involves an electronically excited state of the junction instead of a vibrationally excited state, is discussed *e.g.* in Ref. [33].
- [33] B. D. Fainberg and M. Jouravlev and A. Nitzan, Phys. Rev. B 76, 245329 (2007)

## Figure Captions

Fig.1: Sketch of the model molecular junction for positive ( $\mu_L > 0$ ) and negative ( $\mu_L < 0$ ) bias voltages. The top figures depict the population of electronic levels. Occupied levels in the left (L) and the right (R) lead are represented by the gray-shaded areas. The population of the two electronic states of the molecular bridge, which are represented by two black bars, is indicated by filled and empty circles attached to the respective bars, respectively. Strong (weak) coupling of an electronic state to a lead is indicated by a thick (thin) arched line. The bottom figures give a schematic proposition of a scenario for such a molecular junction. Electron withdrawing ( $R_1, R_2, R_3$ ) and electron donating ( $R_4, R_5, R_6$ ) groups attached to two phenyl rings should induce localization and asymmetric charge distribution of the electronic states, leading to both bias controlled population of the molecular states and bias controlled excitation of the vibrational modes.

Fig.2: Voltage-dependent steady state vibrational excitation, demonstrating mode-selective vibrational excitation in the presence of a moderate coupling to a "cold" bath ( $k_B T = 1 \text{ meV}$ ). The solid, dashed and dot-dashed lines correspond to increasing vibronic coupling. The insets show the respective population of the electronic states. The model parameters are summarized in Table I. The black and colored curves are results of NEGF and density matrix calculations, respectively.

Fig.3 Voltage-dependent mode-selective vibrational excitation in a model with weak coupling to a bath, where nonequilibrium effects prevail. The black and colored curves are results of NEGF and density matrix calculations, respectively. The results have been obtained for a model with two vibrational modes with different (a) and identical (b) frequencies and vibronic coupling strengths, respectively (see Table I for the parameters values).

Fig. 4: Mechanisms of electronic-vibrational energy exchange in molecular junctions. Mechanisms (a) and (b) represent heating and cooling induced by electronic transport between the two leads, respectively. Mechanisms (c) and (d), on the other hand, correspond to cooling by electron-hole pair creation at the left electrode. The thin arrows in (d) reflect the inefficiency of the process due to weak coupling of the unoccupied state to the left lead at positive bias voltages.

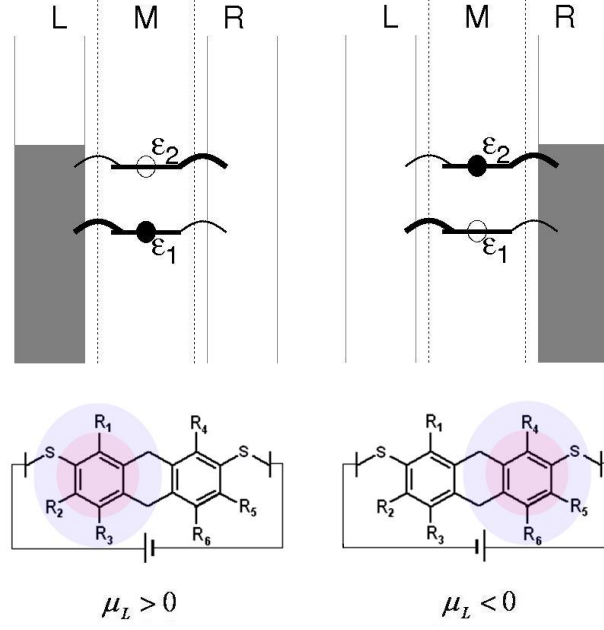


FIG. 1.

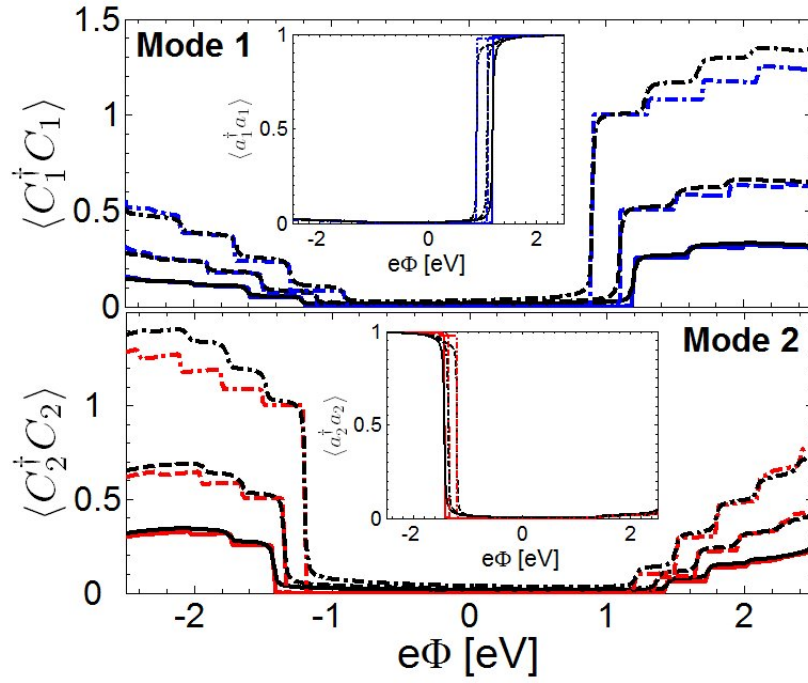


FIG. 2.

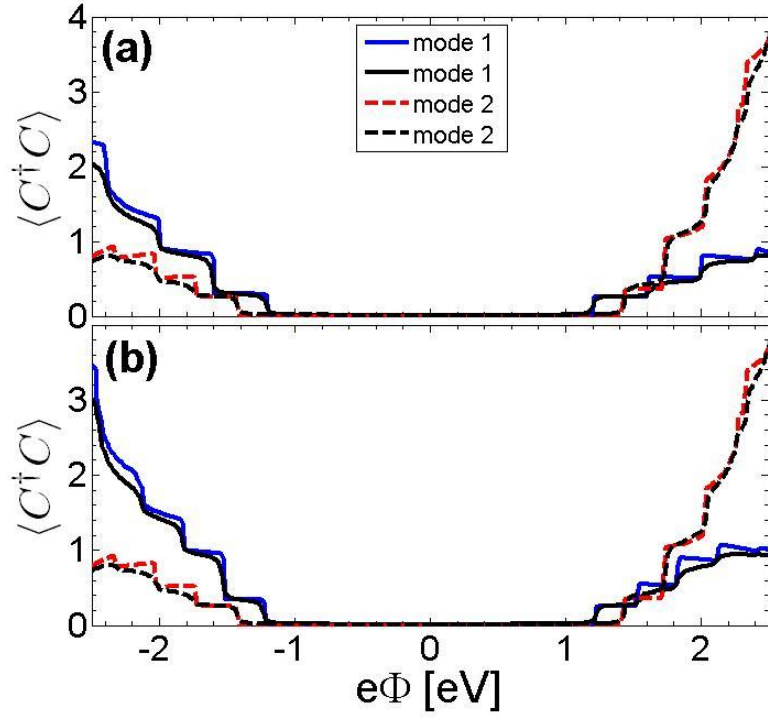


FIG. 3.

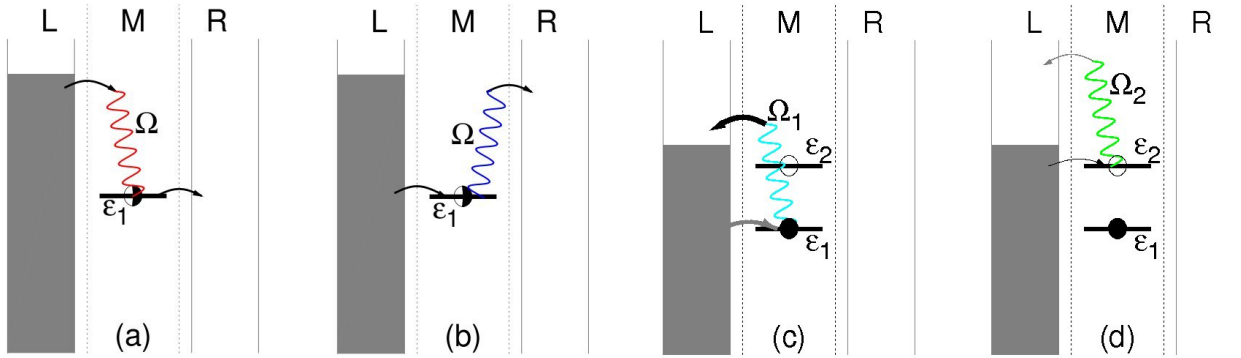


FIG. 4.

TABLE I. Model Parameters (Energy values are in eV)

$\epsilon_1$	$\epsilon_2$	$v_{L,1}, v_{R,2}$	$v_{R,1}, v_{L,2}$	$\omega_{c,1/2}$	$\xi$	$\gamma$	$\Gamma_{L/R}(\mu_{L/R})$	$k_B T$
0.65	0.75	1	0.1	1	-0.1	-1	0.02	0.001
		FIG. 2		FIG. 3a			FIG. 3b	
$\Omega_1$		0.2		0.2			0.15	
$\Omega_2$		0.15		0.15			0.15	
$\frac{\lambda_{1,1}}{\Omega_1}, \frac{\lambda_{2,2}}{\Omega_2}$		$1/\sqrt{2}, 1, \sqrt{2}$		$1/\sqrt{2}$			$1/\sqrt{2}$	
$\zeta_1, \zeta_2$		-0.03		-0.01			-0.01	